Superparamagnetic Relaxation Times for Mixed Cubic and Uniaxial Anisotropy and High Energy Barriers: I. Intermediate-to-High Damping and Uniaxial Axis in a ⟨001⟩ Direction

Andrew J. Newell
*Center for Research in Scientific Computation, Department of Marine, Earth and Atmospheric Sciences, P.O. Box 8208, North Carolina State University, Raleigh, NC 27695-8208**
(Dated: May 5, 2004)

The Néel-Brown theory for superparamagnetic relaxation rates is generalized to ferromagnetic particles with mixed cubic and uniaxial anisotropy. In this article the uniaxial axis is in a ⟨001⟩ crystallographic direction, while in part II it is in a ⟨111⟩ direction. The calculations are for high energy barriers, so transitions between states (stable equilibria) are rare. The approach of Kramers and Brown is used. A master equation is derived assuming that transitions only occur between a given pair of states if the states are directly connected by flux paths across saddle points. The master equation is solved for the probability distribution and the effect on the magnetic moment is calculated. Some relaxation modes have no effect on the moment. There are as many as five distinct relaxation rates for the probability distribution, but at most two for the moment. One rate is for the component parallel to the uniaxial axis while the other is for the perpendicular component. These rates are functions of the cubic anisotropy parameter K_1' and the uniaxial parameter K_u. The double relaxation rate can give rise to phenomena such as partial superparamagnetism and rotation of the moment.

PACS numbers: 76.20+q,75.20.-g

I. INTRODUCTION

The theory of Néel[1], in its original form or the more rigorous theory by Brown[2], has been the main tool for understanding a great variety of thermal relaxation phenomena in ferromagnets. Examples include thermoremanent magnetization (TRM), anhysteretic remanent magnetization (ARM), complex susceptibility and Mössbauer spectra[3–5]. The theory assumes uniaxial anisotropy, which corresponds to full rotational symmetry about a single crystal axis. Uniaxial anisotropy is comparatively easy to work with because the energy depends on only one coordinate. However, no crystal has such a high symmetry, and the expression for the relaxation rate has an anomalous temperature dependence[6]. This drawback is shared by some recent extensions of the Néel-Brown theory[7–10].

Exact expressions for the relaxation rate have also been obtained for pure cubic anisotropy in zero field[11]. However, cubic anisotropy (which is magnetocrystalline) is weak. In general the anisotropy in a real crystal will also have a significant component due to stress or the magnetostatic effect of the shape of the particle. So far, the only attempts to predict the effect of mixed anisotropy have used a quasi-uniaxial approximation[3,12]. This approach is particularly doubtful when the uniaxial anisotropy is small, since it is known that there are multiple relaxation rates for pure cubic anisotropy[13].

In this article and a companion I will calculate zero-field relaxation rates for a mixture of cubic and uniaxial anisotropy. In part I the uniaxial easy axis is in a ⟨001⟩ crystallographic directions, while in part II[14] it is in a ⟨111⟩ direction.

I will use the high energy barrier approximation[13], which assumes that transitions from one magnetic state to another are rare. I will assume intermediate-to-high (IHD) damping. Experimental estimates of the damping parameter have so far been low[15,16]. So why do the IHD case? First, it is too soon to say that all ferromagnets have low damping. Second, the calculations are simpler for the IHD problem, so they provide an opportunity to introduce some of the methods and terminology and to draw some conclusions that are true more generally.

I will explicitly calculate the time dependence of the magnetic moment. Previous authors have often calculated only the time dependence of the probability distribution for the remanent states, implicitly assuming that the moment has the same time dependence. However, this is not generally true. For example, I will show that in the case of pure cubic anisotropy, only one of the three relaxation rates actually affects the moment. More generally, there are separate rates for components parallel to and perpendicular to the uniaxial axis.

II. RELAXATION THEORY

In the high energy barrier approximation[13] energy barriers are high enough that the magnetic state is very likely to be near an energy minimum, so it is meaningful to speak of the probability of being in one of a few discrete states. There can still be enough transitions between states to change the average moment over the time scale of interest. The calculation of relaxation rates can be separated into two parts: calculation of the attempt frequencies between neighboring minima and insertion of all

the frequencies into a master equation.

As in all micromagnetic problems[17], the magnetization has a fixed magnitude equal to the saturation magnetization M_s, and the magnetization vector can be written $\mathbf{M} = M_s\mathbf{m}$, where $\mathbf{m} = (\alpha, \beta, \gamma)$ is a unit vector.

A. Attempt Frequencies Over Barriers

Suppose there are n identical, non-interacting particles with n_i in state i. In the high energy approximation the frequency ν_{ij} of a jump from state i to state j is only nonzero if states i and j are directly connected by a path over a saddle point. In that case, the probability per unit time of a jump from i to j is

$$\nu_{ij} = \nu_{ij}^0 \exp\left[-(g_s - g_i)v/kT\right], \tag{1}$$

where v is the volume of the particle, ν_{ij}^0 is a frequency of the order of the ferromagnetic resonance freqency, g_s is the free energy density at the saddle point and g_i is the energy density of state i.

In the simplest version of the Néel model[1], ν_{ij}^0 is assumed to have a fixed value ν^0 for all the energy barriers. The equilibrium population in state i is then given by the Boltzmann distribution:

$$n_i^{eq} \propto \exp(-g_i v/kT). \tag{2}$$

In effect, this approximation treats each state as a discrete state in which the moment is exactly equal to the moment with energy density g_i.

A more accurate approximation[13], based on Kramers theory, treats the magnetization as continuously varying but with a high probability of being near one of the minima. Let (θ, ϕ) be the spherical coordinates of the unit vector $\mathbf{m}$. For a statistical ensemble of identical particles, suppose that $W(\theta, \phi)d\Omega$ is the probability of $\mathbf{m}$ being within the solid angle $d\Omega$ of the direction (θ, ϕ). In equilibrium, this probability is given by the Boltzmann distribution $W \propto \exp(-gv/kT)$. Choose coordinates such that the z axis is parallel to the moment at the energy minimum. Near the minimum,

$$g \approx g_i + (c_1^{(i)}\alpha_1^2 + c_2^{(i)}\alpha_2^2)/2, \tag{3}$$

where the α_i are the direction cosines perpendicular to the z axis, and $c_1^{(i)}, c_2^{(i)}$ are constants. Near the saddle point,

$$g \approx g_s + (c_1\alpha_1^2 - c_2'\alpha_2^2)/2, \tag{4}$$

where the coordinates are chosen so c_1 and c_2' are both positive.

For state i to be a minimum, $c_1^{(i)}$ and $c_2^{(i)}$ must both be positive. If the probability is sufficiently localized near the minimum, $W \propto \exp(-(c_1^{(i)}\alpha_1^2 + c_2^{(i)}\alpha_2^2)/2kT)$ can be integrated out to infinity to obtain the equilibrium distribution:

$$n_i^{eq} \propto kT\left(c_1^{(i)}c_2^{(i)}\right)^{-1/2}\exp(-g_i v/kT). \tag{5}$$

It is assumed that changes in W are determined by a probability current that is concentrated near the saddle point. This probability current is determined by the dynamics of the individual particles. The time evolution of the moment in a given particle is given by the Landau-Lifshitz equation, which in SI units is

$$\frac{d\mathbf{M}}{dt} = -|\gamma_0'|\mu_0\mathbf{M}\times\mathbf{H}_{\text{eff}} - \frac{|\gamma_0'|\alpha}{M_s}\mu_0\mathbf{M}\times(\mathbf{M}\times\mathbf{H}_{\text{eff}}), \tag{6}$$

where $\mathbf{H}_{\text{eff}} = -\mu_0^{-1}\partial g/\partial\mathbf{M}$ is the effective field, γ_0' is a gyromagnetic parameter in HzT^{-1} and α is a dimensionless damping parameter.

The Kramers theory matches the probability flow out of the minimum to the flow through the saddle point. The resulting expression for the frequency prefactor is[13]

$$\nu_{ij}^0 = G\left(\frac{|\gamma_0'|\alpha}{2\pi M_s}\right)\left(c_1^{(i)}c_2^{(i)}\right)^{1/2}\left(\frac{c_2'}{c_1}\right)^{1/2}, \tag{7}$$

where

$$G = \frac{1}{2c_2'}\left\{(c_2' - c_1) + \left[(c_1 + c_2')^2 + 4\alpha^{-2}c_1c_2'\right]^{1/2}\right\}. \tag{8}$$

In Section III B I will calculate the eigenvalues of the Jacobian for use in the above expressions.

B. Master Equation

Given the attempt frequencies ν_{ij} between each pair of states i and j, the rate of change of n_i is given by the master equation

$$\dot{n}_i = \sum_{i\neq j}\left(\nu_{ji}n_j - \nu_{ij}n_i\right), \tag{9}$$

where the dot denotes time differentiation. For example, a particle with pure uniaxial anisotropy has two states, and their evolution is given by

$$\dot{n}_1 = -\dot{n}_2 = \nu_{21}n_2 - \nu_{12}n_1. \tag{10}$$

In this system the equilibrium distribution ($\dot{n}_i = -\dot{n}_j = 0$) is given by $n_1/n_2 = \nu_{21}/\nu_{12} = 0$. The system decays exponentially towards equilibrium with time constant $(\nu_{12} + \nu_{21})^{-1}$.

In less symmetric systems the minima are connected by a network of saddle points. For example, when the anisotropy is pure cubic with $K_1' > 0$, the minimum-energy directions for the moment are the $\langle 001\rangle$ crystallographic directions, while for the saddle points they are the $\langle 110\rangle$ directions. Because the probability of crossing a given barrier is already low, the probability of jumping

across two barriers at once is ignored. Thus, there is a zero probability of jumping directly from the [001] state to the $[00\bar{1}]$ state because they are only connected by way of other $\langle 001\rangle$ states.

The time evolution can be expressed in matrix form as follows[18]:

$$\dot{\mathbf{n}} = W \cdot \mathbf{n}, \tag{11}$$

where $W_{ij} = \nu_{ji}$ for $i \neq j$ and $W_{ii} = -\sum_j \nu_{ij}$. For the equilibrium equation $\dot{\mathbf{n}} = 0$ to have a solution, the detailed balance condition[19] must be satisfied:

$$W_{ij} n_j = W_{ji} n_i. \tag{12}$$

The detailed balance condition is satisfied for constant prefactor ν_0 if the equilibrium probabilities are given by (2), and for Kramers theory if they are given by (5).

If the detailed balance condition is satisfied, W can be diagonalized[19]:

$$W = V \cdot \Lambda \cdot V^{-1}, \tag{13}$$

where Λ is a diagonal matrix such that Λ_{kk} is the k-th eigenvalue of W, and V is the eigenvector matrix such that column k corresponds to eigenvalue k. The time evolution of $\mathbf{n}$ from an initial state $\mathbf{n}(0)$ is given by[18]

$$\mathbf{n}(t) = V \cdot \mathrm{diag}\left(\exp(\Lambda_{kk} t)\right) \cdot V^{-1} \cdot \mathbf{n}(0), \tag{14}$$

where $\mathrm{diag}\left(\exp(\Lambda_{kk} t)\right)$ is a diagonal matrix with diagonal entries $\Lambda_{kk} t$.

Usually the time dependence of the moment has more physical interest than the probability for each state. This is given by

$$\mathbf{m}(t) = \sum_i n_i(t) \mathbf{m}_i, \tag{15}$$

where $\mathbf{m}_i$ is the moment of state i. This is often simpler than the expressions for $\mathbf{n}(t)$ because many components are eliminated by the symmetry.

III. RESULTS

The calculations are organized as follows. In section III A the equilibrium solution are calculated as functions of the ratio K_u/K_1'. In section III B the eigenvalues of the Jacobian are calculated for each solution are calculated to determine its stability. The eigenvalues are also used to calculate the prefactor for the attempt frequency over each saddle point in section III C. The master equations are constructed in section III D and solved for the time dependence of the probability of each state. Finally, the solutions are used to determine the time dependence of the magnetic moment.

A. Equilibrium Solutions

The first step in calculating the relaxation rates is to identify the stable equilibrium states and determine their energies. Assuming a superposition of cubic anisotopy and uniaxial with rotational axis in the [001] direction, the free energy density is

$$g = K_u(1-\gamma^2) + K_1'(\alpha^2\beta^2 + \beta^2\gamma^2 + \gamma^2\alpha^2), \tag{16}$$

where K_u is the uniaxial parameter and K_1' is the stress-free cubic magnetocrystalline parameter[20].

The uniaxial anisotropy is the sum of contributions from shape anisotropy and inverse magnetostriction. If the particle is rotationally symmetric about some axis and has aspect ratio q, then $K_u = N(q)/2$, where $N(q)$ is the demagnetizing factor[21]. A prolate spheroid has positive K_u and the axis of rotational symmetry is an easy axis for the moment. An oblate spheroid has negative K_u and the rotational axis is a hard axis. If there is a uniaxial stress σ, K_u depends on the crystallographic orientation of the stress and the magnetoelastic parameters λ_{100} and λ_{111}. A uniaxial stress σ in a $\langle 001\rangle$ direction produces a uniaxial easy or hard axis in the same direction with $K_u = (3/2)\lambda_{100}\sigma$. Here, and in the rest of the paper, I use the notation $\langle hkl\rangle$ to indicate all the states that are equivalent by cubic symmetry to $[hkl]$.

In the expansion for cubic anisotropy I have left out the second order term $K_2\alpha^2\beta^2\gamma^2$. This is generally small, and it is unlikely that K_1' and K_u will both be so small that K_2 matters. A larger source of potential error is the assumption that the non-magnetocrystalline anisotropy is uniaxial. In general it will be triaxial, but that would add greatly to the difficulty of the calculation. The anisotropy is often nearly uniaxial, and the anomalous temperature dependence mentioned in the introduction disappears because the cubic anisotropy breaks the rotational symmetry. For the calculations in this article the physical origin of the parameter K_u is not important, and I will simply take K_u as given. For completeness, I will calculate relaxation rates for both prolate ($K_u < 0$) and oblate ($K_u > 0$) uniaxial anisotropy.

Equilibrium solutions for this problem are stationary points of the free energy with the constraint $\mathbf{m}\cdot\mathbf{m} = 1$. Using this constraint, we can make the substitution $\gamma^2 = 1 - \alpha^2 - \beta^2$ in (16). Then g depends only on α and β. Taking the derivatives with respect to these variables, and assuming $K_1' \neq 0$, we obtain the equilibrium equations

$$2\alpha\left[\kappa + 1 - 2\alpha^2 - \beta^2\right] = 0 \tag{17a}$$

$$2\beta\left[\kappa + 1 - \alpha^2 - 2\beta^2\right] = 0, \tag{17b}$$

where $\kappa = K_u/K_1'$. The solutions to these equations are then substituted into $\gamma = \pm(1-\alpha^2-\beta^2)^{1/2}$ to get $\mathbf{m}$. Not all the equilibrium solutions are obtained from the above equations, but the remaining solutions can be obtained either by invoking the symmetry or by successive substitutions for α and β in g. The solutions are given in Table I.

TABLE I: General solutions for uniaxial axis in the [001] direction. The left column gives the name I will use to refer to each solution. The components are for the unit vector in the direction of the moment. The eigenvalues are for the Jacobian of the energy in coordinates such that the z axis is in the direction of the moment.

Name	Components	g/K_1'	J_i/K_1'
u	$(0,0,\pm1)$	0	$2(1+\kappa)$ (double)
100	$(\pm1,0,0),(0,\pm1,0)$	κ	$2, 2(1-\kappa)$
110	$2^{-1/2}(\pm1,\pm1,0)$	$\kappa+\frac{1}{4}$	$1-2\kappa, -2$
0ab	$(\pm a,0,\pm b),(0,\pm a,\pm b)^a$	$\frac{1}{4}(1+\kappa)^2$	$1+\kappa, 2(\kappa^2-1)$
ccd	$(\pm c,\pm c,\pm d)^b$	$\frac{1}{3}(1+\kappa)^2$	$\frac{4}{3}(1+\kappa)(-1+2\kappa)$, $-\frac{4}{3}(1+\kappa)$

[a]Where $a=\sqrt{(1+\kappa)/2}$ and $b=\sqrt{(1-\kappa)/2}$.
[b]Where $c=\sqrt{(1+\kappa)/3}$ and $d=\sqrt{(1-2\kappa)/3}$.

B. Stability

The solutions to (17) include all the minima, maxima and saddle points. In this section I will determine their stability by calculating the eigenvalues of a Jacobian of the energy, taking into account the constraint $\mathbf{m}\cdot\mathbf{m}=1$. This is best done in coordinates perpendicular to the magnetization vector because the eigenvalues can also be used in the Kramers theory (section II A). If $m_i^\perp$ are the coordinates in a suitably rotated reference frame, then $\mathbf{m}=R^\perp\cdot\mathbf{m}^\perp$. Substituting for $\mathbf{m}$ in (16) and substituting $\gamma^\perp=\sqrt{1-(\alpha^\perp)^2-(\beta^\perp)^2}$ results in a free energy in terms of the perpendicular coordinates $\alpha^\perp$ and $\beta^\perp$. The Jacobian is obtained by calculating the derivatives in terms of $\alpha^\perp$ and $\beta^\perp$ and substituting $\alpha^\perp=\beta^\perp=0$.

For the u state R is just the identity. For other states, one can use the matrix

$$R_{ij}^\perp=\begin{pmatrix} ac/\sqrt{a^2+b^2} & -b/\sqrt{a^2+b^2} & a \\ bc/\sqrt{a^2+b^2} & a/\sqrt{a^2+b^2} & b \\ -\sqrt{a^2+b^2} & 0 & c\end{pmatrix}. \tag{18}$$

The eigenvalues of the Jacobian are given in Table I. Each solution is a minimum if both eigenvalues are positive, a maximum if both are negative, and a saddle point if one is positive and one negative. In addition, the 0ab solutions are only real if $|\kappa|<1$, while the ccd solutions are only real if $-1<\kappa<1/2$.

C. Single-Barrier Attempt Frequencies

The attempt frequencies that will be needed in the master equations are listed in Table II. They are defined by the starting point (an energy minimum) and the barrier (a saddle point) over which the jump occurs. These frequencies are also labeled in Figs. 2-5. The coefficients that are needed in equations 7 and 8 are listed in Table II.

In addition, values of γ_0' and α are needed. We can express γ_0' in terms of $\gamma_0=g\mu_B/2\hbar$ (where μ_B is the Bohr magneton and $g\approx2$ the gyromagnetic factor) as follows. The parameter γ_0 appears in the Gilbert equation

$$\frac{d\mathbf{M}}{dt}=-|\gamma_0|\mu_0\mathbf{M}\times\left(\mathbf{H}_{\text{eff}}-\eta\frac{d\mathbf{M}}{dt}\right), \tag{19}$$

where η is a dissipation parameter. This equation is equivalent to the Landau-Lifshitz equation[13] with $|\gamma_0'|=|\gamma_0|/(1+\gamma_0^2\eta^2\mu_0^2M_s^2)$ and $\alpha=|\gamma_0|\eta\mu_0M_s$. Thus,

$$|\gamma_0'|=|\gamma_0|/(1+\alpha^2). \tag{20}$$

In the high damping limit ($\alpha\gg1$),

$$\nu^0\approx\left(\frac{|\gamma_0|}{2\pi M_s\alpha}\right)\left(c_1^{(i)}c_2^{(i)}\right)^{1/2}\left(\frac{c_2'}{c_1}\right)^{1/2}. \tag{21}$$

The c parameters depend on K_1' and K_u.

By contrast, the prefactor for uniaxial anisotropy is[13]

$$\nu^0=\frac{\alpha}{1+\alpha^2}\frac{2|\gamma_0|K_u^{3/2}v^{1/2}}{M_s(\pi kT)^{1/2}}. \tag{22}$$

It depends on particle volume and has an explicit dependence on temperature. Thus, the expression for mixed cubic and uniaxial anisotropy does not approach (22) as K_u increases. This is to be expected as the cubic anisotropy does not disappear. However, it also does not approach (22) as K_1' goes to zero. This mismatch occurs because the assumptions behind the Kramers theory break down. The saddle point is nearly flat perpendicular to the direction of flow, so probability flow is not restricted to the neighborhood of a saddle point. Because of the high symmetry of the uniaxial case, an asymptotic expansion would be needed to bridge the gap.

The prefactors, normalized by $2\pi M_s/|\gamma_0K_1'|$, are plotted in Fig. 1 for iron and nickel. The normalized prefactor is dimensionless and depends only on α, κ and the sign of K_1'. Near the values $\kappa=-1$, 0.5 and 1, the prefactors generally diverge. Again, this is an indication that the assumptions behind the Kramers model are breaking down. The model depends on the assumption that there is quasi-equilibrium in a small region around each minimum and saddle point. Brown[13] suggests the condition that the second order term $\exp(-(c_1\alpha_1^2+c_2\alpha_2^2)v/2kT)$ must become negligibly small while α_1 and α_2 are still small. This condition fails near the critical values of κ because one or more of the c coefficients goes to zero as states appear or disappear (Table II).

D. Master Equations

The form of the master equation is determined by the topology of the network connecting energy minima across saddle points. In this section the master equations are formulated and solved for each topology. Using the single-barrier attempt frequencies ν_i as input variables, I solve the master equation analytically following

TABLE II: Single-barrier attempt frequencies ν_i. Each frequency is defined by the starting minimum and the saddle point that is crossed. The table lists energy barriers and coefficients in the expansions (3 and 4) of the energy near the minimum and saddle point. These coefficients are the eigenvalues from section III B, except that the negative eigenvalue for the saddle point is made positive to get c_2'. All parameters are normalized by $|K_1'|$.

ν	min	saddle	$c_1^{(1)}$	$c_1^{(2)}$	c_1	c_2'	$(g_s - g_i)$
ν_1	100	110	2	$2-2\kappa$	$1-2\kappa$	2	$\frac{1}{4}$
ν_2	u	110	$-2-2\kappa$	$-2-2\kappa$	2	$1-2\kappa$	$-\kappa-\frac{1}{4}$
ν_3	u	0ab	$2+2\kappa$	$2+2\kappa$	$1+\kappa$	$2-2\kappa^2$	$\frac{1}{4}(1+\kappa)^2$
ν_4	100	0ab	$2-2\kappa$	$2-2\kappa$	$1+\kappa$	$2-2\kappa^2$	$\frac{1}{4}(1-\kappa)^2$
ν_5	ccd	0ab	$\frac{4}{3}(1+\kappa)(1-2\kappa)$	$\frac{4}{3}(1+\kappa)$	$2-2\kappa^2$	$1+\kappa$	$\frac{1}{12}(1+\kappa)^2$
ν_6	ccd	110	$\frac{4}{3}(1+\kappa)(1-2\kappa)$	$\frac{4}{3}(1+\kappa)$	2	$1-2\kappa$	$\frac{1}{12}(2\kappa-1)^2$
ν_7	110	0ab	$2\kappa-1$	2	$2-2\kappa^2$	$1+\kappa$	$-\frac{1}{4}\kappa(\kappa-2)$
ν_8	u	100	$2+2\kappa$	$2+2\kappa$	2	$2\kappa-2$	κ
ν_9	110	100	$2\kappa-1$	2	$2\kappa-2$	2	$\frac{1}{4}$

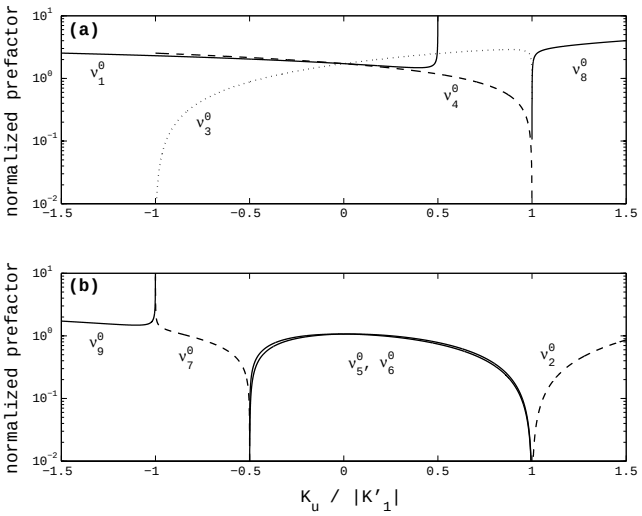

FIG. 1: Prefactors for the single-barrier relaxation rates ν_i. (a) $K_1' > 0$. (b) $K_1' < 0$. The damping parameter α is set to 0.1 and the prefactors are normalized by $2\pi M_s/|\gamma_0 K_1'|$.

the method of Section II B. The values for the ν_i can be substituted in the solution to obtain the relaxation rate.

The number of each type of solution (minimum, saddle point or maximum) must satisfy the topological constraint[22]

$$\#\text{max} - \#\text{saddle} + \#\text{min} = 2, \tag{23}$$

as long as all of the solutions are isolated (it does not apply to pure uniaxial anisotropy because the maximum is a great circle rather than a point). This criterion is related to the more familiar Euler's theorem for polyhedra: $V - E + F = 2$, where V is the number of vertices, E of edges and F of faces. For convenience, I will use V, E, F to represent the number of minima, saddle points and maxima.

I organize this section by the value of κ because that determines the equilibrium solutions. There are then two networks of stable states, depending on the sign of K_1'. If κ is kept fixed and the sign of K_1' is changed, the eigenvalues of the Jacobian change sign. This converts maxima into minima and vice versa while leaving saddle points as saddle points. These changes leave $V - E + F$ unchanged.

The calculations in this section were implemented using the MATLAB® Symbolic Toolbox. I have provided the script in the electronic supplement.

1. $\kappa < -1$

For $\kappa < -1$ and $K_1' > 0$, there are four 100 minima, four 110 saddle points and two u maxima (Fig. 2). Thus, the topological constraint $V-E+F = 2$ is satisfied. Each 100 minimum is connected to two nearest neighbors by a 110 saddle point. Therefore,

$$\nu_{ij} = \begin{bmatrix} 0 & 0 & \nu_1 & 0 \\ \nu_1 & 0 & \nu_1 & 0 \\ 0 & \nu_1 & 0 & \nu_1 \\ \nu_1 & 0 & \nu_1 & 0 \end{bmatrix}, \tag{24}$$

where ν_1 is labeled in Fig. 2 and defined in Table II. The eigenvalues of W_{ij} are

$$\lambda_i = (-4\,\nu_1, -2\,\nu_1, -2\,\nu_1, 0) \tag{25}$$

and the corresponding eigenvector matrix is

$$V_{ij} = \begin{bmatrix} -1 & -1 & 0 & 1 \\ 1 & 0 & -1 & 1 \\ -1 & 1 & 0 & 1 \\ 1 & 0 & 1 & 1 \end{bmatrix}. \tag{26}$$

The last column corresponds to the zero eigenvector. Its components are therefore proportional to the number of particles in each state in equilibrium.

Not all transitions affect the moment. Let us label the states so the $+x$ direction is state 1. Then the first

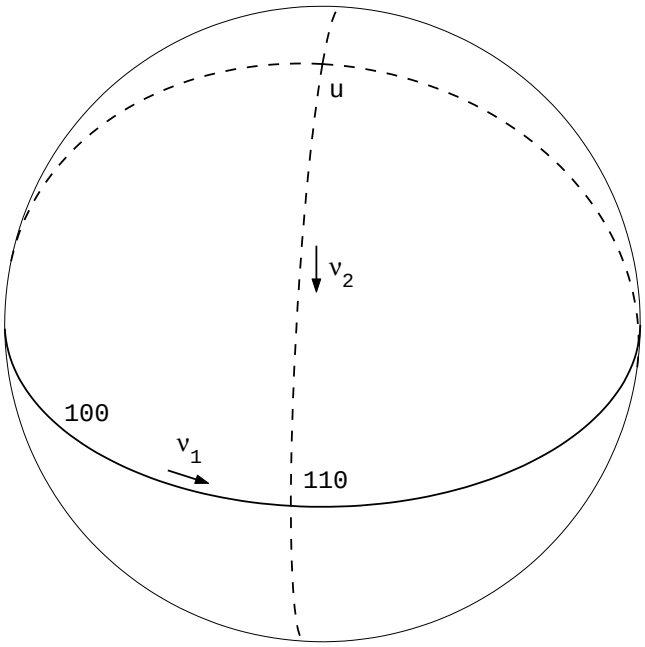

FIG. 2: Equilibrium states and their connections for $K_1' > 0$, $\kappa = -3/2$ and easy axis in the [001] direction. The viewpoint is close to the [111] direction. The streamlines of the energy gradient through the saddle points are shown as solid lines if they connect with minima and dashed lines if they connect with maxima. Rates across the energy barriers are indicated with labels and arrows. If $K_1' < 0$ dashed and solid lines are exchanged, maxima are exchanged with minima and saddle points remain the same.

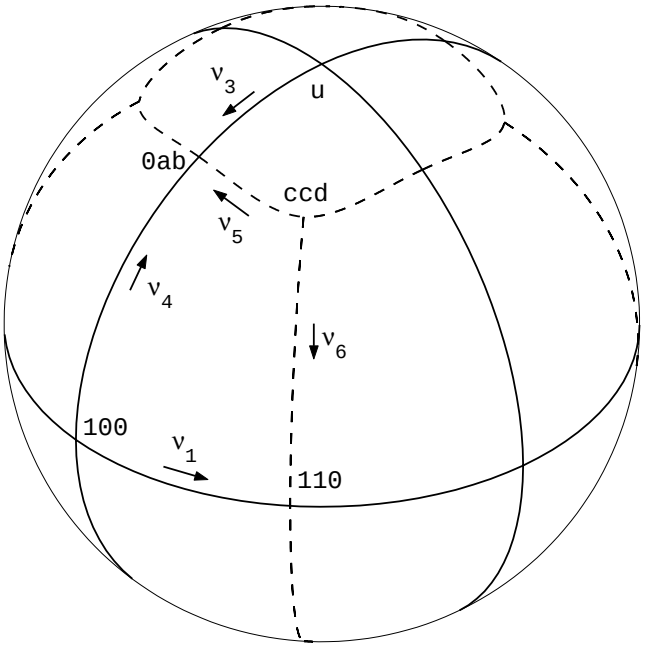

FIG. 3: Equilibrium states and their connections for $K_1' > 0$, $\kappa = -1/2$ and easy axis in the [001] direction. The conventions are the same as for Fig. 2.

eigenvector corresponds to transitions from the x to the y axis. Along a given axis, the populations in both directions change equally, so the moment is unaffected. By contrast, the second and third eigenvectors correspond to transitions from one end of the x or y axis to the other, so they do affect the moment. Both of these eigenvectors have eigenvalue $-2\nu_1$.

Assume all the particles are initially in state 1. Then $\mathbf{n}(0) = (1, 0, 0, 0)^T$. The time evolution of the moment can be determined using (14-15) with $\Lambda_{ii} = \lambda_i$. The result is that the moment remains in the $+x$ direction and decays with rate $2\nu_1$. Thus, the component $\mathbf{m}_\perp$ perpendicular to the uniaxial axis has time dependence

$$\mathbf{m}_\perp(t) = \mathbf{m}_\perp(0) \exp(-2\nu_1 t), \tag{27}$$

while the parallel component $m_\parallel$ is identically zero. Equivalently, the perpendicular relaxation rate is ($\nu_\perp = 2\nu_1$) while the parallel rate ($\nu_\parallel$) is undefined.

If $K_1' < 0$ the two u states are minima connected by four 110 saddle points. The moment is therefore always in the u direction and

$$m_\parallel(t) = m_\parallel(0) \exp(-8\nu_2 t). \tag{28}$$

The perpendicular component is identically zero. Thus, $\nu_\parallel = 8\nu_2$ and $\nu_\perp$ is undefined.

2. $-1 < \kappa < 1/2$

When κ crosses -1 the u state bifurcates (Fig. 3). Newly formed 0ab and ccd states start near the z axis for $\kappa = -1$ and travel towards the x and y axes as κ increases. The 100 and 110 states remain the same. For $K_1' > 0$ the u and 100 states are minima, the ccd states are maxima and the 0ab and 110 states are saddle points. Thus, $V - E + F = 6 - 12 + 8 = 2$. The nearest-neighbor connections form an octahedron with each vertex corresponding to a minimum and each edge to a saddle point. Number the minima so that the first is $(0, 0, 1)$, the next four are the 100 states, and the last is $(0, 0, -1)$. Then

$$\nu_{ij} = \begin{bmatrix} 0 & \nu_3 & \nu_3 & \nu_3 & \nu_3 & 0 \\ \nu_4 & 0 & \nu_1 & 0 & \nu_1 & \nu_4 \\ \nu_4 & \nu_1 & 0 & \nu_1 & 0 & \nu_4 \\ \nu_4 & 0 & \nu_1 & 0 & \nu_1 & \nu_4 \\ \nu_4 & \nu_1 & 0 & \nu_1 & 0 & \nu_4 \\ 0 & \nu_3 & \nu_3 & \nu_3 & \nu_3 & 0 \end{bmatrix}. \tag{29}$$

The eigenvalues of W are

$$\begin{aligned} \lambda_i = (&-4\,\nu_3 - 2\,\nu_4, -4\,\nu_3, -2\,\nu_4 - 4\,\nu_1, \\ &-2\,\nu_4 - 2\,\nu_1, -2\,\nu_4 - 2\,\nu_1, 0). \end{aligned} \tag{30}$$

The relaxation depends on whether the initial state is u or 100. If it is u, the parallel relaxation rate is $\nu_\parallel = 4\nu_3$ and the perpendicular rate is undefined. If the initial state is 100, $\nu_\parallel$ is undefined and $\nu_\perp = 2(\nu_1 + \nu_4)$. As in

the previous section, not all relaxation modes affect the moment. For example, it is clear from Fig. 3 that from a 100 state jumps are equally likely to the [001] and $[00\bar{1}]$ states, so ν_4 cannot appear in $\nu_\parallel$. However, jumps can occur between 100 states by way of either u state, so ν_4 does appear in $\nu_\perp$.

If $K_1' < 0$ the ccd states are minima connected by 110 and 0ab saddle points. The geometry is that of a cube, with the eight vertices being ccd states. Number the states so the first four are in the $+z$ hemisphere and state $i+4$ is in the opposite direction to state i. Then

$$\nu_{ij} = \begin{bmatrix} 0 & \nu_5 & 0 & \nu_5 & 0 & 0 & \nu_6 & 0 \\ \nu_5 & 0 & \nu_5 & 0 & 0 & 0 & 0 & \nu_6 \\ 0 & \nu_5 & 0 & \nu_5 & \nu_6 & 0 & 0 & 0 \\ \nu_5 & 0 & \nu_5 & 0 & 0 & \nu_6 & 0 & 0 \\ 0 & 0 & \nu_6 & 0 & 0 & \nu_5 & 0 & \nu_5 \\ 0 & 0 & 0 & \nu_6 & \nu_5 & 0 & \nu_5 & 0 \\ \nu_6 & 0 & 0 & 0 & 0 & \nu_5 & 0 & \nu_5 \\ 0 & \nu_6 & 0 & 0 & \nu_5 & 0 & \nu_5 & 0 \end{bmatrix}. \qquad (31)$$

The matrix W has five distinct eigenvalues.

All of the remanent states are the same type (ccd), so we can determine the time evolution of the moment by looking at any one remanent state. The relaxation rates are $\nu_\parallel = 2\nu_6$ (with initial component $m_\parallel(0) = d = \sqrt{(1-2\kappa)/3}$) and $\nu_\perp = 2\nu_5$ (with initial component $m_\perp(0) = c = \sqrt{(1+\kappa)/3}$).

3. $1/2 < \kappa < 1$

As κ approaches 1/2 from below, two ccd states converge on each 110 state and are annihilated, changing the stability of the 110 state (Fig. 4). For $K_1' > 0$ there are six minima (the 100 and u states), eight 0ab saddle points and four 110 maxima. The minima are still numbered as for $-1 < \kappa < 1/2$, but now there are no connections between the 100 states. The relaxation rates are therefore obtained by setting ν_1 equal to zero. The rates are $\nu_\parallel = 4\nu_3$ and $\nu_\perp = 2\nu_4$.

If $K_1' < 0$ the 110 states are minima, each connected to each of two neighbors by two 0ab saddle points. Thus, the moment is restricted to the (001) plane. The time dependence of the moment is obtained as for $\kappa < -1$ and $K_1' > 0$, replacing ν_1 by $2\nu_7$. Thus, $\nu_\perp = 4\nu_7$ and $\nu_\parallel$ is undefined.

4. $\kappa \geq 1$

When κ crosses 1 the 0ab states merge with the 100 states (Fig. 5). The geometry is that of Fig. 2 rotated by an angle of $\pi/4$ about the z axis, so the same derivations

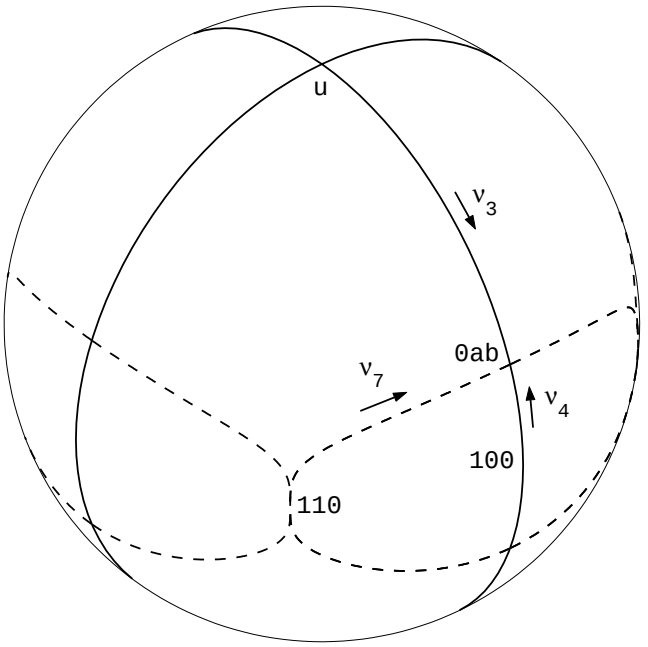

FIG. 4: Equilibrium states and their connections for $K_1' > 0$, $\kappa = 3/4$ and easy axis in the [001] direction. The conventions are the same as for Fig. 2.

TABLE III: Relaxation rates in terms of the single-barrier rates ν_i.

κ	$K_1' > 0$		$K_1' < 0$	
	$\nu_\parallel$	$\nu_\perp$	$\nu_\parallel$	$\nu_\perp$
$(-\infty, -1)$	—	$2\nu_1$	$8\nu_2$	—
$(-1, 1/2)$	$4\nu_3$ [a]	$2(\nu_1+\nu_4)$ [b]	$2\nu_6$ [c]	$2\nu_5$ [d]
$(1/2, 1)$	$4\nu_3$ [a]	$2\nu_4$ [b]	—	$4\nu_7$
$(1, \infty)$	$2\nu_8$	—	—	$2\nu_9$

[a] Initial state is u and $\nu_\perp$ is undefined.
[b] Initial state is 100 and $\nu_\parallel$ is undefined.
[c] Initial component is $d = \sqrt{(1-2\kappa)/3}$.
[d] Initial component is $c = \sqrt{(1+\kappa)/3}$.

can be used for the relaxation rates. Thus, for $K_1' > 0$ we get $\nu_\parallel = 2\nu_8$ and $\nu_\perp$ is undefined. For $K_1' < 0$, $\nu_\parallel$ is undefined and $\nu_\perp = 2\nu_9$.

IV. DISCUSSION

I showed in section III D that in general there are two relaxation rates, one parallel ($\nu_\parallel$) and one perpendicular ($\nu_\perp$) to the uniaxial axis. The rates are compiled in Table III.

When $\kappa = 0$ (pure cubic anisotropy) and $K_1' > 0$ then $\nu_1 = \nu_3 = \nu_4 \equiv \nu$, where

$$\nu = G\left(\frac{|\gamma_0'|\alpha\sqrt{2}}{\pi M_s}\right) K_1' \exp\left(-\frac{K_1' v}{4kT}\right) \qquad (32)$$

and $G = 1/4 + (1/4)(9 + 8\alpha^{-2})^{1/2}$. The relaxation rates

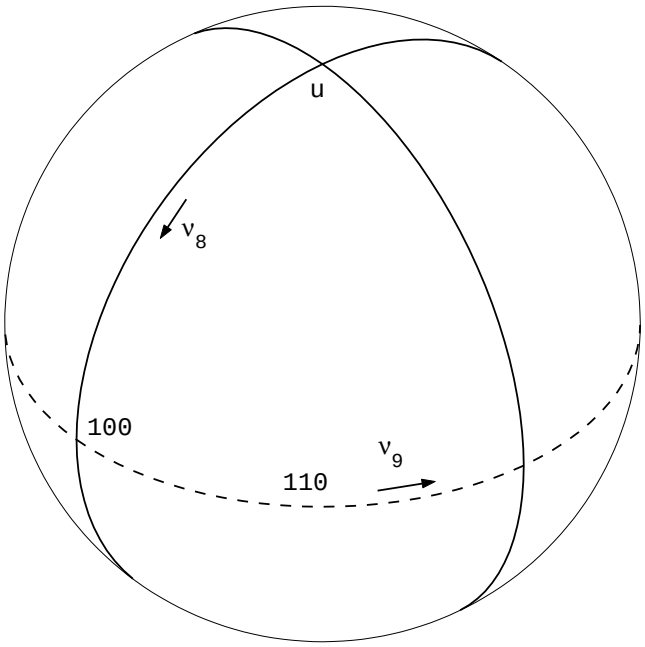

FIG. 5: Equilibrium states and their connections for $K_1' > 0$, $\kappa = 5/4$ and easy axis in the [001] direction. The conventions are the same as for Fig. 2.

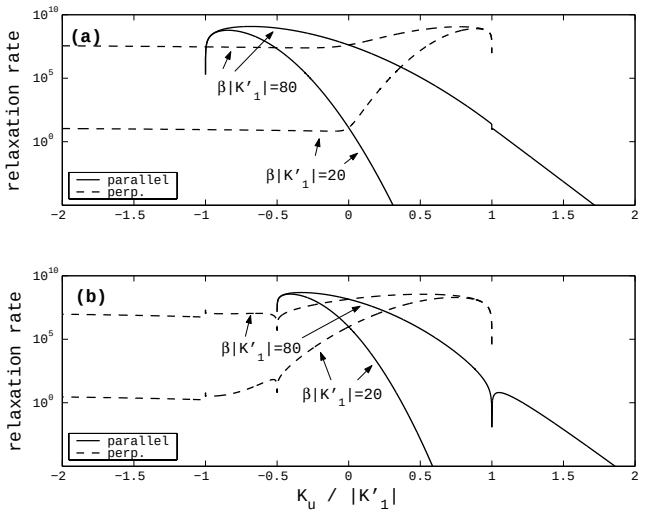

FIG. 6: Relaxation rates for (a) Fe ($M_s = 1.72 \times 10^6\,\mathrm{kA/m}$, $K_1' = 4.8 \times 10^4\,\mathrm{Jm^{-3}}$) and (b) Ni ($M_s = 4.85 \times 10^5\,\mathrm{kA/m}$, $K_1' = -5 \times 10^3\,\mathrm{Jm^{-3}}$). Solid lines are $\nu_\parallel$ and dashed lines are $\nu_\perp$. Two values of $\beta|K_1'|$ are shown, where $\beta = v/kT$. The damping parameter α is set to 0.1.

for the probability distribution are 4ν and 6ν. This agrees with previous theory[13]. However, $\nu_\parallel = \nu_\perp = 4\nu$, so only one relaxation rate affects the magnetic moment.

When $\kappa = 0$ and $K_1' < 0$ then $\nu_5 = \nu_6 \equiv \nu$, where

$$\nu = G\left(\frac{|\gamma_0'|\alpha\sqrt{2}}{\pi M_s}\right)|K_1'|\exp\left(-\frac{|K_1'|v}{12kT}\right) \qquad (33)$$

and $G = 1/2 + (1/2)(9 + 8\alpha^{-2})^{1/2}$. The relaxation rates for the probability distribution are $2\nu, 4\nu$ and 6ν, again in agreement with previous theory[13]. However, $\nu_\parallel = \nu_\perp = 2\nu$, so only one of the three relaxation rates affects the moment.

For $K_1' > 0$ and $-1 < \kappa < 1$, the rate $\nu_\parallel = 4\nu_3$ (corresponding to jumps over 0ab barriers from u states) has the same energy barrier as Dormann et al.[3] used in their quasi-uniaxial approximation. We now see that the approximation is valid for $|\kappa| < 1$, but only for relaxation parallel to the uniaxial axis. Since many of the states have a large perpendicular moment, perpendicular relaxation can have as great or greater effect on the moment.

Relaxation rates for iron and nickel are shown in Fig. 6 for two values of v/kT. A function for calculating the rates is included in the electronic supplement. The value of $|\gamma_0|$ is[23] 1.8×10^{11} $\mathrm{HzT^{-1}}$. Measurements for α are between about 0.005 and 0.05[15,16]. Since this may lie in the low-dissipation regime, I have chosen a larger value of 0.1 for α.

The divergences in prefactor, discussed in Section III C, are apparent in Fig. 6. Although they indicate a breakdown in the assumptions behind the Kramers theory, the problem appears to be restricted to very near the three critical values of κ. All the rates approach zero at the ends of the curves. This is reasonable because some state is disappearing, and near the end its Boltzmann probability will approach zero. The discontinuities in the middle of the curves are probably not real. The true probabilities and probability currents should change smoothly with K_u and K_1'. Thus, the correct curve can be estimated by smoothing the curves across the discontinuities.

The existence of two relaxation rates is a qualitative departure from the Néel-Brown theory with implications for many of the applications such as thermoremanent magnetization. Because the rates can differ by several orders of magnitude, many measurements will only detect one rate, while others will see no relaxation at all. The vast difference in time scales will present a very difficult resolution problem for numerical models of stochastic dynamics.

A less obvious implication is that a particle may be partly superparamagnetic. On time scales between the two rates, equilibrium exists within certain clusters of states but not between clusters. For example, in Fig. 3 with $K_1' < 0$, states with a positive z component would be in equilibrium with each other. Such a cluster has a nonzero average moment, so it can carry a remanence, but the remanence will be reduced by thermal fluctuations. The two relaxation rates are for different directions in a particle, so in an oriented sample the partial remanence will also be rotated.

The particles modeled in this article are single-domain. The number of available states tends to increase with particle size. Even in an elongated particle with no magnetocrystalline or magnetoelastic anisotropy, new states with moments perpendicular to the long axis appear as

the size increases[24]. Thus, multiply connected states, and multiple relaxation times, are probably the rule in larger particles.

Acknowledgments

This research was supported by Grants EAR-0208446 (Earth Sciences Division of the National Science Foundation) and NAG5-13465 (NASA Exobiology Program).

---

* Andrew_Newell@ncsu.edu; http://www4.ncsu.edu/~ajnewell/index.html

[1] L. Néel, Ann. Géophys. **5**, 99 (1949), translated in Nicholas Kurti, editor, *Selected Works of Louis Néel*, Gordon and Breach, New York, 1988, pages 407–427.

[2] W. F. Brown, Jr., Phys. Rev. **130**, 1677 (1963).

[3] J. L. Dormann, D. Fiorani, and E. Tronc, Adv. Chem. Phys. **98**, 283 (1997).

[4] D. J. Dunlop and O. Özdemir, *Rock Magnetism: Fundamentals and Frontiers* (Cambridge Univ. Press, New York, 1997), 573 pp.

[5] R. Egli and W. Lowrie, J. Geophys. Res. **107**, 2209 (2002).

[6] I. Klik and L. Gunther, J. Stat. Phys. **60**, 473 (1990).

[7] A. Aharoni, Phys. Rev. **177**, 793 (1969).

[8] W. T. Coffey, D. S. F. Crothers, Y. P. Kalmykov, E. S. Massawe, and J. T. Waldron, Phys. Rev. E **49**, 1869 (1993).

[9] W. T. Coffey, D. S. F. Crothers, Y. P. Yalmykov, and J. T. Waldron, Phys. Rev. B **51**, 15947 (1995).

[10] D. A. Garanin, Phys. Rev. E **54**, 3250 (1996).

[11] Y. P. Yalmykov, S. V. Titov, and W. T. Coffey, Phys. Rev. B **58**, 3267 (1998).

[12] A. J. Newell and R. T. Merrill, J. Geophys. Res. **104**, 617 (1999).

[13] W. F. Brown, Jr., IEEE Trans. Magn. **MAG-15**, 1196 (1979).

[14] A. J. Newell (2004), submitted to Physical Review B.

[15] T. J. Silva, C. S. Lee, T. M. Crawford, and C. T. Rogers, J. Appl. Phys. **85**, 7849 (1999).

[16] T. J. Silva and T. M. Crawford, IEEE Trans. Magn. **35**, 671 (1999).

[17] W. F. Brown, Jr., *Micromagnetics* (Interscience, New York, 1963), (Reprinted by Krieger, New York, 1978.) 143 pp.

[18] T. Moon and R. T. Merrill, Phys. Earth Planet. Inter. **34**, 186 (1984).

[19] N. G. van Kampen, *Stochastic Processes in Physics and Chemistry* (North-Holland, New York, 1981), 419 pp.

[20] J. Ye, A. J. Newell, and R. T. Merrill, Geophys. Res. Lett. **21**, 25 (1994).

[21] S. Chikazumi, *Physics of Ferromagnetism* (Oxford, New York, 1997), 655 pp.

[22] V. I. Arnold, *Ordinary Differential Equations* (MIT Press, Cambridge, MA, 1973), translated and edited by R. A. Silverman. 280 pages.

[23] P. J. Mohr and B. N. Taylor, Rev. Mod. Phys. **72**, 351 (2000).

[24] A. J. Newell and R. T. Merrill, J. Geophys. Res. **105**, 19377 (2000).

*